

## Supplemental Information

### 5-methylcytosine recognition by *Arabidopsis thaliana* DNA glycosylases DEMETER and DML3

Sonja C. Brooks, Robert L. Fischer, Jin H. Huh, and Brandt F. Eichman\*

Mutant	$k_{st}$ 5mC-DNA	Relative to WT	$k_{st}$ 5hmC-DNA	Relative to WT	$k_{st}$ 5caC-DNA	Relative to WT	$k_{st}$ T/G-DNA	Relative to WT
F759A	4.0 ± 0.2	0.2	4.3 ± 2.0	0.5	16 ± 5	1.9	3.2 ± 0.2	0.5
T776A	11.2 ± 0.2	0.6	3.5 ± 0.1	0.4	6.0 ± 1.6	0.7	7.7 ± 0.3	0.7
D781A	ND	0	ND	0	21 ± 4	2.5	ND	0
H1360A	ND	0	ND	0	ND	0	ND	0
Y1361F	10.9 ± 0.4	0.6	4.4 ± 0.3	0.5	17 ± 3	2	3.7 ± 0.2	0.6
I1364A	ND	0	ND	0	7.1 ± 1.7	1.1	10 ± 2	1.5

First-order single-turnover rate constants ( $k_{st}$ , x  $10^{-5}$  s $^{-1}$ ) for excision of oxidized 5mC nucleobases from a 25mer oligonucleotide at 25 °C, pH 8.5 and 170 mM ionic strength. Values represent the averages and standard deviations from at least three experiments. ND, no detectable activity.

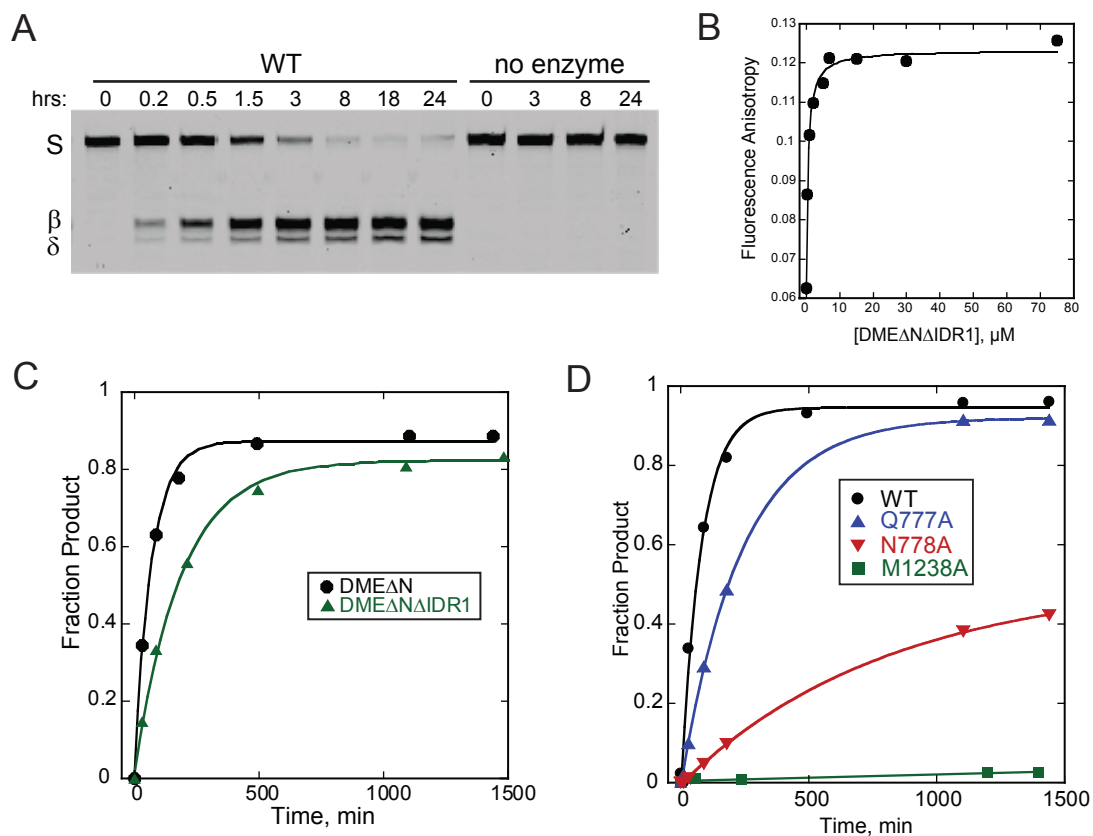


**Fig. S1. 5mC excision kinetics and DNA binding of DME.** (A) Representative denaturing polyacrylamide gel showing DNA glycosylase activity. Reactions contained FAM-5mC-DNA and either 17 μM or 0 μM DMEΔNΔIDR1. Numbers above the gel represent reaction times in hours. Substrate (S) and β and δ elimination products are labeled. (B) Representative fluorescence anisotropy binding isotherm for wild-type DMEΔNΔIDR1 binding to 25mer 5mC-DNA. (C) 5mC excision activities of DMEΔN (black circles) and DMEΔNΔIDR1 (green triangles) under non-saturating conditions (2 μM protein). (D) 5mC excision activities of plug and wedge mutants compared to DMEΔNΔIDR1 (WT) used to determine single-turnover rates ( $k_{st}$ ) shown in Table 1.

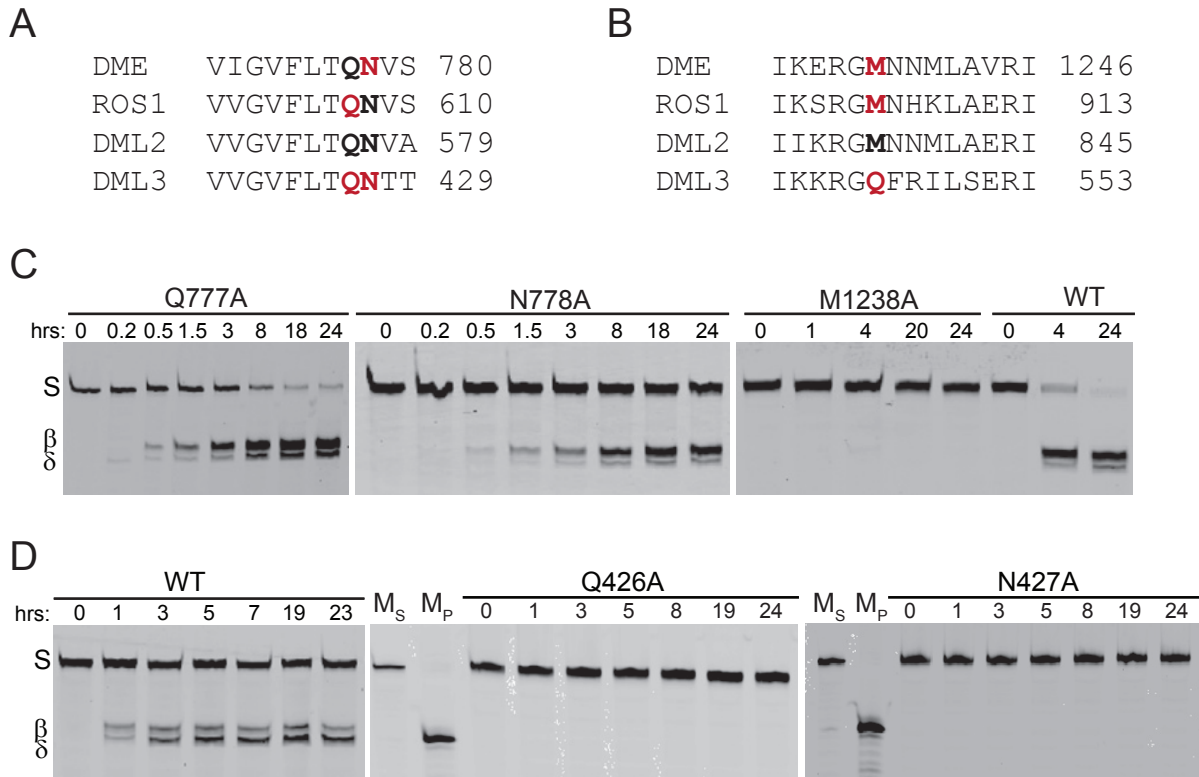


**Fig. S2. Identification of DNA intercalation residues in DME and DML3.** (A,B) Sequence alignments of the regions containing the plug (A) and wedge (B) DNA intercalating residues. Residues predicted and confirmed by mutagenesis to intercalate DNA are boldface and red, respectively. (C,D) Base excision activity of DME $\Delta$ N $\Delta$ IDR1 (C) and DML3 $\Delta$ N (D) point mutants. Numbers above the gels represent the reaction times in hours. M<sub>s</sub>, molecular weight standard for 25mer substrate; M<sub>p</sub>, molecular weight standard for 12mer product.

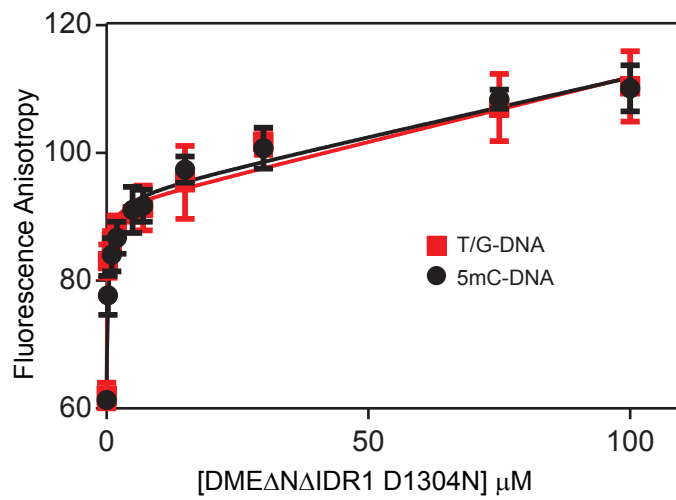


**Fig. S3. Binding to 5mC- and T/G-DNA.** Fluorescence anisotropy binding isotherm for catalytic mutant DME $\Delta$ N $\Delta$ IDR1 D1304N binding to 25mer 5mC-DNA (black circles) and T/G-DNA (red squares). Data was fit using a wo-state binding model in GraphPad Prism 6.

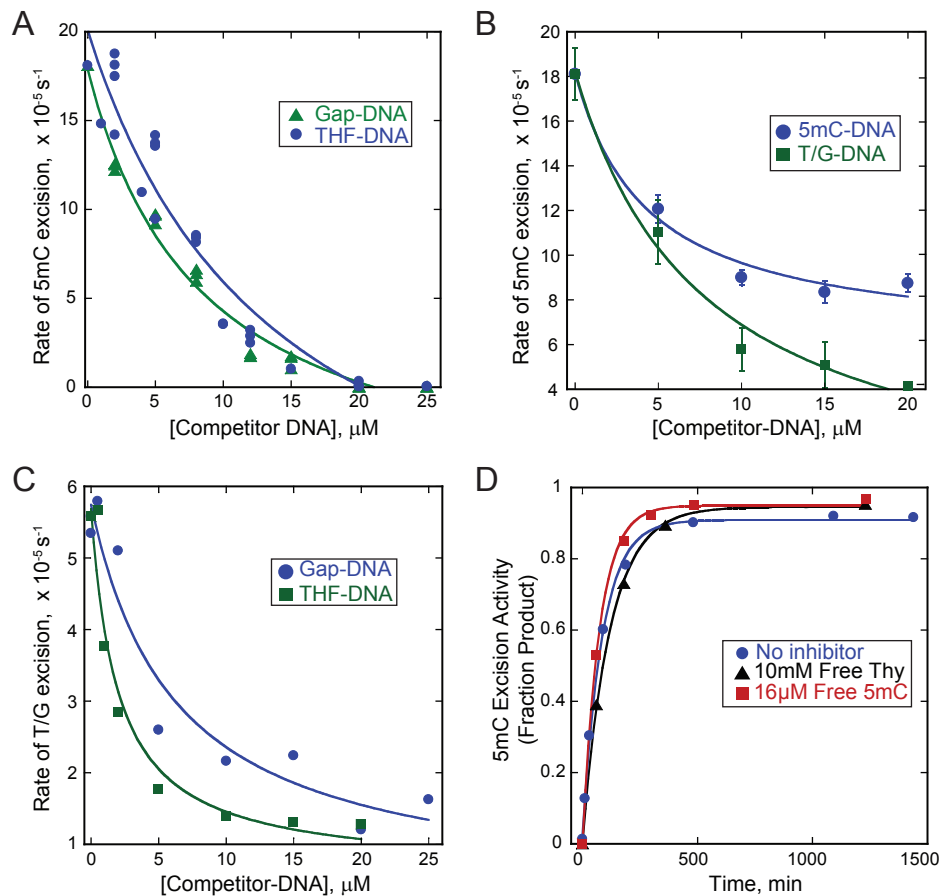


**Fig. S4. Inhibition of 5mC and T/G excision by reaction intermediates.** (A,B) Rate constants for reactions containing 10 µM DMEΔNΔIDR1, 100 nM radiolabeled 5mC-DNA, and indicated amounts of cold 25-mer competitor DNA duplex containing a 1-nucleotide gap or tetrahydrofuran (THF) abasic site mimetic (A), or containing 5mC- or T/G substrates (B). (C) Rate constants for T/G excision by 2 µM DMEΔNΔIDR1 incubated with 100 nM radiolabeled T/G-DNA in the presence of the indicated amounts of Gap- and THF-DNA. (D) 5mC excision activity for 10 µM DMEΔNΔIDR1 incubated with 100 nM radiolabeled 5mC-DNA in the presence of 16 µM 5mC or 10 mM thymine.

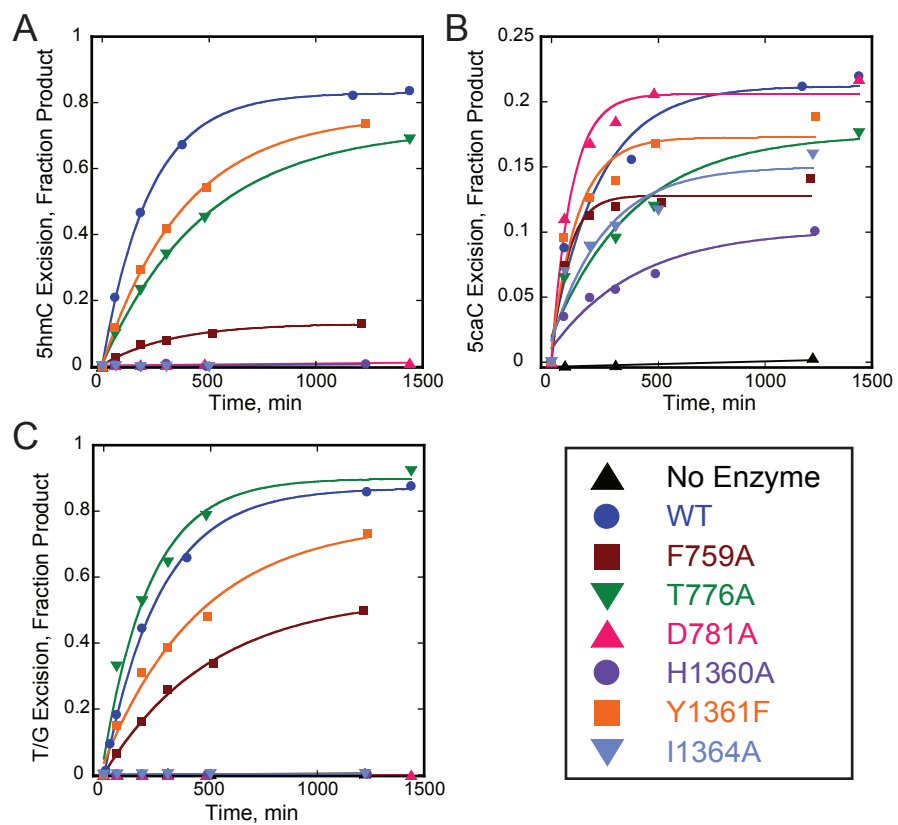


**Fig. S5. 5hmC, 5caC, and T/G excision kinetics.** Single-turnover excision rates of 5hmC (A), 5caC (B), and T/G (C) by active site mutants compared with wild-type (WT) DME $\Delta$ N $\Delta$ IDR1.